The upper frequency limit of dynamic cerebral autoregulation

Ronney B. Panerai[1,2], Thompson G. Robinson[1,2], Jatinder S. Minhas[1,2]

[1]*Cerebral Haemodynamics in Ageing and Stroke Medicine (CHIASM) Research Group, Department of Cardiovascular Sciences, University of Leicester, Leicester, LE2 7LX, UK*

[2]*National Institute for Health Research Leicester Biomedical Research Centre, University of Leicester, Leicester, LE3 9QP, UK*

Correspondence:
Dr Jatinder S. Minhas
Department of Cardiovascular Sciences,
Leicester, United Kingdom
Phone: +44 116 2523134
Email: jm591@le.ac.uk
ORCID ID JS Minhas: 0000-0002-0576-9105, Twitter: @DrJMinhas

Abbreviated title: Upper frequency limit of dCA
Pages: 31
Tables: 2
Figures: 5
Key words: Cerebral Circulation, Frequency, Autoregulation, Hemodynamics

This is an Accepted Article that has been peer-reviewed and approved for publication in the The Journal of Physiology, but has yet to undergo copy-editing and proof correction. Please cite this article as an 'Accepted Article'; doi: 10.1113/JP278710.

KEY POINTS SUMMARY

- Dynamic cerebral autoregulation (CA) is expressed by the temporal pattern of cerebral blood flow (CBF) recovery following a sudden change in arterial blood pressure (BP).
- Transfer function analysis of BP as input and CBF velocity (CBFV) as output can express dynamic CA through its amplitude (or gain) and phase frequency responses.
- The upper frequency limit (F_{upLim}) at which dynamic CA can operate is of considerable physiological interest and can also provide additional information about worsening CA due to disease processes.
- In healthy subjects F_{upLim} was strongly dependent on $PaCO_2$ changes induced by four different breathing manoeuvres.
- The considerable inter-subject variability in F_{upLim} suggests that fixed frequency bands should not be adopted for averaging values of gain and phase in studies of dynamic CA.

ABSTRACT

Dynamic cerebral autoregulation (CA) can be expressed in the frequency domain by the amplitude and phase frequency responses calculated by transfer function analysis (TFA) of arterial blood pressure (BP) and cerebral blood flow velocity (CBFV). We studied the effects of $PaCO_2$ on the upper frequency limit (F_{upLim}) of these responses and its inter-subject variability. Twenty-four healthy subjects (11 female, age 36.0 ± 13.4 years) were recruited. Recordings of CBFV (transcranial Doppler ultrasound), BP (Finometer) and end-tidal CO_2 ($EtCO_2$, capnography) were performed during five minutes at rest (normocapnia), and during four breathing manoeuvres: 5% and 8% CO_2 in air and hyperventilation targeting reductions of 5 and 10 mmHg compared to normocapnia. F_{upLim} was determined by the break point of the Autoregulation Index (ARI) curve as a function of frequency when the phase response was gradually set to zero. The five breathing conditions led to highly significant differences in $EtCO_2$ ($p<0.0001$), CBFV ($p<0.0001$), ARI ($p<0.0001$) and F_{upLim} ($p<0.0001$). F_{upLim} ranged from 0.167 ± 0.036 Hz at the lowest values of hypocapnia (28.1 ± 1.9 mmHg) to 0.094 ± 0.040 Hz at the highest level of hypercapnia (41.7 ± 5.4 mmHg), showing a correlation of $r=-0.53$ ($p<0.001$) with $EtCO_2$. These findings reinforce the key role of $PaCO_2$ in CBF regulation. The considerable inter-subject variability of F_{upLim} suggests that fixed frequency bands should not be adopted for averaging values of gain and phase in dynamic CA studies, and that the higher frequency band (0.20-0.40) Hz in particular, does not contain relevant information about dynamic CA. Further investigations are needed to assess the information value of F_{upLim} as a marker of dynamic CA efficiency in physiological and clinical studies.

INTRODUCTION

Under normal physiological conditions, the cerebral circulation is protected from large excursions in arterial blood pressure (BP) by the mechanism of cerebral autoregulation (CA), that tends to maintain cerebral blood flow (CBF) approximately constant (Paulson et al., 1990). Although the pioneering work of Lassen (1959) indicated the presence of a CBF plateau in the BP range of 60-150 mmHg, more recent work suggests that the BP range might be much narrower, with the absence of a flat plateau (Heistad & Kontos 1983; Willie *et al.*, 2014; Drummond, 2019). Classical studies of CA were based on measurement techniques that averaged data over several minutes. More recently, noninvasive methods such as transcranial Doppler ultrasound (TCD) and finger arterial volume clamping have allowed recordings of BP and CBF velocity (CBFV) with much higher temporal resolution, leading to the distinction between 'static' and 'dynamic' autoregulation (Aaslid *et al.*, 1989; Tiecks *et al.*, 1995). Whilst the former is often characterised by the well-known schematic CA curve with a plateau, the latter can provide the transient response of CBFV to sudden changes in mean BP, induced by manoeuvres, such as the sudden release of inflated thigh cuffs, or due to spontaneous fluctuations (Aaslid *et al.*, 1989; Tzeng & Panerai, 2018; Simpson & Claassen, 2018)

Different approaches have been adopted to model the dynamic relationship between BP and CBF aiming to improve our understanding of CA physiology, as well as deriving parameters that could characterise the strength of dynamic CA in health and disease (Panerai, 2008). From a physiological perspective, approaches based on spontaneous fluctuations in BP and CBF have been regarded as ideal, due to the lack of interference from autonomic, sensorimotor or cognitive processes, resulting from BP manipulation, that could interfere with the intrinsic mechanisms of dynamic CA (Tzeng & Panerai, 2018), despite concerns about its reliability (Simpson & Claassen, 2018). With this approach, studies of dynamic CA have been dominated by transfer function analysis (TFA), adopting BP as the *input* variable and CBF (usually estimated as CBFV) as the corresponding *output* (Claassen *et al.*, 2016). Since its inception, TFA studies of dynamic CA have described it as a 'frequency-dependent' phenomenon, characterized by the amplitude ('gain') and phase frequency responses (Giller, 1990; Panerai *et al.*, 1996a; Zhang *et al.*, 1998). One additional frequency-dependent parameter, the coherence function, determines the reliability of gain and phase estimates at each frequency (Giller, 1990) and its tendency to present relatively low values for frequencies

below 0.07 Hz, have led to the proposal to break down the frequency range of dynamic CA into three distinct bands, that is the very low frequency (VLF, 0.01-0.07 Hz), low frequency (LF, 0.07-0.20 Hz) and high frequency (HF, 0.20-0.40 Hz) bands (Zhang *et al.*, 1998; Claassen *et al.*, 2016).

Both theoretical principles and empirical observations, lead to the conclusion that there is a maximum frequency at which dynamic CA can respond to changes in BP. This becomes clear from visual inspection of gain and phase frequency responses (Panerai *et al.*, 1996b; Zhang *et al.*, 1998; Panerai *et al.*, 2002; Sammons *et al.*, 2007), as well as from transient responses induced by very rapid changes in BP (Aaslid *et al.*, 1989; Tiecks *et al.*, 1995). Although the HF band is generally assumed not to contain relevant information about dynamic CA, the use of a fixed upper frequency limit for the LF band of 0.20 Hz is problematic for two main reasons. First, this frequency was never justified or validated on physiological grounds, and second, it suggests that the 0.2 Hz limit is not phenotype dependent, which is unlikely. When studying the frequency limits of dynamic CA, it is essential to take into consideration the key role of $PaCO_2$ on CBF regulation (Hoiland *et al.*, 2019). An extensive literature demonstrates that both static and dynamic CA are attenuated by hypercapnia whilst hypocapnia leads to upregulation. However, not enough attention has been paid to the influences of $PaCO_2$ on the speed of the CBF response to sudden changes in BP (Aaslid *et al.*, 1989; Panerai *et al.,* 1999; Minhas *et al.*, 2018), which should be expected to be directly related to the upper frequency limit of dynamic CA. To address the questions above, we adopted a robust procedure to identify the upper frequency limit of dynamic CA in healthy subjects at rest, aiming to test two specific hypotheses: i) the upper frequency limit of dynamic CA is not a fixed quantity but shows considerable variation across a healthy population, and ii) the upper frequency limit of dynamic CA is dependent on $PaCO_2$.

METHODS

Subjects and measurements

All study procedures were conducted in accordance with the Declaration of Helsinki (2000). The University of Leicester Ethics Committee (Reference: jm591-c033) provided ethical approvals for this study. Healthy volunteers were recruited from University departmental staff, students and their relatives. Healthy volunteers 18 years and over were included. Individuals with physical disease in the upper limb, poor insonation of both temporal bone

windows and any significant history of cardiovascular, neurological or respiratory disease were excluded. Written informed consent was obtained from all participants prior to any study activities being conducted. In a previous study the same dataset was used to describe the feasibility of modelling cerebrovascular variables using a logistic model (Minhas *et al.*, 2018).

The University of Leicester's Cerebral Haemodynamics in Ageing and Stroke Medicine research laboratory was the setting for the study, a quiet area maintained at approximately 24°C. Study participants were requested to avoid exercise, caffeine, alcohol and nicotine in the 12-hour period before study measurements. Heart rate (HR) was recorded using a standard 3-lead electrocardiogram (ECG). Beat-to-beat BP was recorded continuously using the Finometer® device (FMS, Finapres Measurement Systems, Arnhem, Netherlands), which was attached to the middle finger of the left hand. The hand bearing the finger cuff was at the level of the heart to negate any hydrostatic pressure artefact. $EtCO_2$ was measured throughout the initial resting baseline and hypercapnic phase using a face-mask connected to a capnograph (Capnocheck Plus). During the second baseline and hypocapnic phase, $EtCO_2$ was measured via nasal prongs (Salter Labs). Bilateral insonation of the middle cerebral arteries (MCAs) was performed using transcranial Doppler (TCD) ultrasound with a 2MHz probe (Viasys Companion III; Viasys Healthcare). A head-frame was used to secure the probes in position and adjusted to ensure maximum comfort for study participants. In order to accurately identify the MCAs, careful assessment of signal depth and velocities was undertaken (Aaslid *et al.*, 1982).

Experimental protocol

All measurements were conducted at a single visit with randomization of the order of hypo- and hypercapnia, determined in advance using a random number generator. Initially, a stabilization period of 15 minutes of measurement whilst resting and supine was undertaken. This was followed by CO_2 inspiration in air, with a face mask, constantly ('fixed inspiration') for a minimum of 90 s with a randomized order of 5% CO_2 or 8% CO_2. A steady 90 s recording was conducted before each gas inspiration episode to ensure systemic haemodynamic stability before and immediately after the hypercapnic challenge. After a further stabilization period of 5 minutes, participants performed another resting supine recording prior to hyperventilation in random order, at different respiratory rates, generating

incremental reductions in $EtCO_2$ of 5mmHg and 10mmHg less than normocapnia for that individual. Hyperventilation was sustained for a minimum period of 90 s. For hyperventilation, participants were asked to breathe with a metronome (KORG Metronome MA-30) creating a respiratory rate of at least 5 breaths per minute above their resting rate for at least 90 s. Two-minute washout periods of normal respiration were allowed between successive measurements. Each incremental reduction in $EtCO_2$ was repeated on two occasions during the same session. The repeat assessments were not averaged, the first was designed to be a trial assessment to determine the ability to achieve the target $EtCO_2$, this was then formally assessed on the second occasion. The rationale for using the above $EtCO_2$ targets for hypocapnia and percentages of CO_2 in air for hypercapnia, were based on previous studies in our laboratory, demonstrating that these thresholds lead to significant changes in CBFV and CA metrics (Panerai *et al.*, 1999; Minhas *et al.*, 2018; Minhas *et al.*, 2019).

Measurements were continuously recorded at a rate of 500 samples/s in the PHYSIDAS data acquisition system (Department of Medical Physics, University Hospitals of Leicester). Systolic and diastolic brachial BP readings (OMRON Model 705IT) were performed at each stage of the protocol (normocapnia, hypercapnia and hypocapnia with a minimum of three recordings per individual). These values were then used to calibrate the Finometer recordings.

Data Analysis

Six individual files were generated for each participant: 2 at baseline, 2 hypercapnic and 2 hypocapnic. Data were visually inspected and calibrated to recorded OMRON systolic and diastolic BP values. After removal of narrow spikes (<100ms) by linear interpolation, the CBFV recording was passed through a median filter. Then signals were low pass filtered with a zero-phase Butterworth filter with a 20Hz frequency cut-off. The QRS complex of the electrocardiogram (ECG) was automatically detected and marking of the R-R interval was visually checked. This permitted mean BP, HR, $EtCO_2$ and mean CBFV to be calculated for each cardiac cycle. $EtCO_2$ was detected at end expiration, linearly interpolated, and synchronised to the cardiac cycle.

Transfer function analysis (TFA), adopting mean BP values as input and CBFV as output, was performed according to CARNet's White Paper recommendations (Claassen *et al.*, 2016). Multiple segments of data lasting 102.4 s (512 samples) were used to estimate the auto- and cross-spectra, based on Welch's method, adopting a 50% superposition of

segments. The auto-spectra was expressed as power spectral densities (PSD). Estimates of gain and phase were accepted at each frequency for statistically significant values of coherence, using its 95% confidence limit, taking into account the degrees of freedom of estimates (Claassen *et al.*, 2016). The CBFV response to a hypothetical step change in mean BP was obtained by performing the inverse Fourier transform of the entire gain and phase frequency responses, and then integrating the impulse response (Panerai, 2004). The CBFV step response was compared to each of the 10 template responses proposed by Tiecks et al (Tiecks *et al.*, 1995) and the corresponding Autoregulation Index (ARI) was obtained from the curve with the least mean square error (MSE), subjected to strict statistical criteria for acceptance, requiring a mean value of coherence in the frequency range 0.15-0.25 Hz above the 5% confidence limit and the normalised MSE < 0.30 (Panerai *et al.*, 2016). Values of ARI=0 represent absence of autoregulation, whilst ARI=9 corresponds to the most efficient CA that can be observed.

Detection of the upper frequency limit (F_{upLim}) of dynamic CA followed a robust procedure based on the key role of the phase frequency response of the BP-CBFV relationship. Accumulated evidence indicates that dynamic CA is a phase-determined mechanism, due to the non-linear relationship resulting from the way myogenic control of vascular smooth muscle changes cerebrovascular resistance (Hughson *et al.*, 2001). It is possible to demonstrate that the TFA amplitude frequency response is superfluous, when expressing the effectiveness of dynamic CA (Panerai, 2008), which possibly explains the differences in reliability between phase and gain when used to assess deterioration of dynamic CA in clinical conditions (Panerai, 2008). From these properties of the phase frequency response, the F_{upLim} could be expressed by the frequency at which the phase reaches zero (Fig. 1), as this value would indicate the absence of dynamic CA. As indicated in Fig. 1 though, in this frequency region, estimates of phase tend to oscillate around the zero value making it fairly difficult to obtain an accurate value of F_{upLim}. To overcome this difficulty, an alternative approach was adopted, by gradually zeroing the phase response, starting from the maximal available frequency (0.5 Hz) (Claassen *et al.*, 2016) and then calculating the corresponding value of ARI at each frequency. This procedure generates an ensemble of ARI values that are frequency dependent [*ARI(f)*], as represented in Fig 2.C. For frequencies above F_{upLim}, the CBFV responses (Fig. 2.A), and corresponding values of *ARI(f)* (Fig. 2.C) are unaffected, but as significant values of phase start to be zeroed, the CBFV step responses and values of

ARI(f) indicate a trend towards worse dynamic CA, with a distinctive 'break point' that we defined as the F_{upLim} value. Fig. 2 also illustrates the corresponding changes in CBFV step responses and *ARI(f)* when, instead of the phase, the gain frequency pattern is destroyed, by gradually replacing values of gain, from f=0.5 Hz, down to 0.01 Hz, by its value at the first harmonic. The technical reasons why the gain spectrum is destroyed with constant values, instead of zeroing it, will be discussed later, but as shown in Figs 2.B and 2.D, in this representative subject neither the CBFV step responses nor the *ARI(f)* series were significantly affected by destroying the frequency pattern of gain, instead of phase, thus confirming the dominant role of phase to inform estimates of F_{upLim}. Similar behaviour was observed in all subjects.

Statistical analysis

Parametric or non-parametric tests were adopted following the result of the Shapiro-Wilk W statistic. Repeated measures paired (dependent t-test or Wilcoxon matched-pair) or multigroup (two-way ANOVA or Friedman) were used for testing for the effects of hemisphere and/or $PaCO_2$ levels. For the latter, five distinct conditions were considered: normocapnia (from the first baseline recording), two levels of hypercapnia (5% and 8% CO_2 in air), and two levels of hypocapnia (hyperventilation targeted at -5 mmHg and -10 mmHg below normocapnia). Association between parameters were expressed with the correlation coefficient (Pearson's or Spearman rank test). Bonferroni correction of p-values was adopted for the case of multiple comparisons. A segmental, bi-linear regression was implemented to estimate F_{upLim} from the *ARI(f)* ensemble (Fig. 2.C). Under visual control, markers were placed around the region likely to show the two break points shown in Fig. 2.C. The breakpoint at higher frequencies (F_{upLim}) could be seen in all recordings, but many *ARI(f)* curves also showed a second breakpoint at lower frequencies that needed to be taken into account to optimise the bi-linear regression. For this purpose, a two-dimensional optimisation procedure was adopted to minimise the total mean square error (MSE) of both regressions, using a range of frequencies of ±0.05 Hz around the initial marker placed under visual inspection. Therefore, to identify the optimal position of the two breakpoints, the overall minimum MSE was chosen from an 11x11 matrix of different combinations of univariate linear regressions. Inter-hemisphere differences were tested for bi-lateral parameters (CBFV, ARI, F_{upLim}) and averaged between the right and left sides if non-significant. The influence of

sex was tested with the mixed-effects model and by comparing slopes between separate linear regressions of F_{upLim} as a function of $EtCO_2$ for males and females.

A value of $p<0.05$ was adopted as the criterion of statistical significance.

RESULTS

Good quality recordings were obtained in 41 subjects, but due to the strict conditions imposed on the acceptance of estimates of ARI (Panerai *et al.*, 2016), complete sets of 10 values (two hemispheres, five levels of $PaCO_2$) were only obtained in 24 individuals (11 female) with mean (SD) age 36.0 (13.4) years. In these subjects, the five distinct breathing conditions led to highly significant differences in $EtCO_2$ and CBFV, without differences in BP or HR (Table 1).

Inter-hemispherical differences in CBFV, ARI and F_{upLim} were not significant for each breathing condition (paired t-test) and were averaged in further statistical analyses. Nevertheless, in Fig. 3, population averages of the *ARI(f)* curve are shown separately for the two MCAs, for the five breathing conditions, indicating a broad association between the F_{cutLim} breakpoint and the step changes in $EtCO_2$. As values of $EtCO_2$ increased from hyperventilation (-10 mmHg target) to hypercapnia (8% CO_2 in air), the *ARI(f)* curve was shifted down and the mean F_{upLim} point was moved towards lower values (Fig. 3, Table 2). Corresponding standard values of ARI (with intact phase spectrum) were also markedly reduced with increasing values of $EtCO_2$ (Table 2). Both the ARI and F_{upLim} showed highly significant differences (ANOVA $p<0.0001$) for the five breathing conditions (Fig. 3, Table 2). Post-hoc analysis (Tukey) revealed that F_{upLim} values for both levels of hypocapnia were different from normocapnia ($p<0.01$) and hypercapnia ($p<0.0002$), but the latter did not show other inter-condition differences.

The association between F_{upLim} and $EtCO_2$ was confirmed by a Pearson's correlation coefficient of $r=-0.53$ ($p<0.001$), involving data from all five breathing conditions. Separate linear regressions for males and females (Fig. 4) did not show differences between slopes ($p=0.108$) and this was confirmed by the non-significant effect of sex in the mixed-effects model ($p=0.99$). Five values of *ARI(f)*, at the highest level of hypercapnia, had values of standard ARI=0. In these cases, corresponding values of F_{upLim} could not be estimated, leading to 63 values for males and 52 values for females in Fig. 4. The correlation of F_{upLim}

with standard values of ARI was r=0.37 (p=0.004), but this association became non-significant when the influence of $EtCO_2$ was removed in multiple regression analysis, explained by the strong association between ARI and $EtCO_2$ (r=-0.49, p=0.001).

The dependence of F_{upLim} on $PaCO_2$ could result from changes in BP and/or CBFV variability, provoked by the different breathing conditions imposed to induce hypo- and hypercapnia. However, the PSD distributions shown in Fig. 5 suggest that this was not the case as the shifts in F_{upLim} were not related to the amount of BP and CBFV power at each frequency.

DISCUSSION

Main findings

Although dynamic CA is generally regarded as a frequency-dependent phenomenon, its upper frequency limit has not been previously reported in humans. The highly consistent values of F_{upLim} that we found within each breathing condition showed coefficients of variation (SD/mean, Table 2) ranging from 21.6% (incremental reductions in $EtCO_2$ of 10mmHg) to 42.5% (8% hypercapnia), thus indicating that F_{upLim} has considerable inter-subject variability and cannot be assumed to be a fixed quantity. This finding suggests that our first hypothesis should be accepted. Moreover, the strong association found between F_{upLim} and $EtCO_2$ (Figs. 3 & 4, Table 2) also suggests acceptance of our second hypothesis. Taken together, these findings indicate that assessment of dynamic CA could benefit from an expanded representation of its effectiveness, by considering the entire *ARI(f)* curve in each individual, instead of the standard, uni-dimensional ARI parameter. Incorporating F_{upLim} as a parameter to be considered in further studies of cerebrovascular physiology and pathology has a number of other implications as discussed below.

Physiological considerations

Differently from biological phenomena that can show frequency responses in the range of kHz, such as nerve and muscle electrical activity, cerebrovascular control mechanisms, like dynamic CA or the baroreceptor reflex, have their frequency response limited by the periodicity of the cardiac cycle. In humans, CA responses taking place within a single cardiac cycle have not been demonstrated. In fact, it takes several heart beats to observe CBFV returning to its original level when BP is disturbed by the sudden release of compressed thigh

cuffs or other manoeuvres (Aaslid *et al.*, 1989). Although heart rate can be highly variable, between individuals and also physiological conditions, frequency-domain analyses of cerebro- and cardiovascular phenomena usually assume a standard heart rate of 60 bpm, thus leading to a sample frequency of 1 Hz for parameters derived from each cardiac cycle. As established by Nyquist's Theorem (Bendat & Piersol, 1986), the maximum frequency content that can be observed is half the sampling frequency and for this reason the spectra is normally only expressed up to a limit of 0.5 Hz. Nevertheless, this limitation is not critical, as most cardiovascular control mechanisms operate at lower frequencies, such as the baroreceptor response, the sympathetic control of blood vessels or the interaction between respiration and heart rate (Cooke *et al.*, 1999; Karemaker, 1999; Zhang *et al.*, 2001). From our results, the highest frequencies achieved for the dynamic CA response were observed with the most strenuous hyperventilation aimed at reducing $EtCO_2$ by 10 mmHg compared to normocapnia. Assuming a gaussian distribution for F_{upLim}, from the values in Table 2, one would expect the highest frequency to be around approximately 0.24 Hz. This estimate has methodological implications for assessment of dynamic CA in humans, to be discussed below, but also raises the question about which effectors are limiting the speed of response. Going from the fastest to the slower phenomena involved in a sudden change in mean BP leading to changes in vessel diameter, one could propose that vascular smooth muscle (VSM) contraction would be the 'bottleneck' for the speed of response. From nerve and muscle electrophysiology, ionic channel permeabilities and membrane excitability are known to be much faster phenomena. Transmission of mean BP changes to arterioles would take place from one cardiac cycle to the next, and would thus be manifested at frequencies well above 0.24 Hz. Moreover, the identification of VSM as the limiting factor on the speed of response, also provides a more consistent explanation for the influences of $PaCO_2$ on F_{upLim} (Figs. 3 & 4, Table 2). Changes in $PaCO_2$, resulting from different breathing conditions, did not change mean BP or HR (Table 1), but, as expected, led to changes in CBFV, reflecting the well-known effects of $PaCO_2$ on small vessel diameter. Our findings agree with the seminal study of Aaslid *et al.* (1989) showing that the speed of the CBFV response to sudden changes in BP is increased by hypocapnia and slowed down by hypercapnia. Two main pathways could be advanced to explain why $PaCO_2$ had such strong influence on F_{upLim}. Firstly, with vasodilation, VSM needs a greater amount of shortening to achieve the same reduction in flow. From the extremes of hypocapnia to hypercapnia (Table 1), CBFV increased by 40%. Assuming a single vessel model, characterised only by vascular resistance, from the fourth power

dependence on vessel radius (Pouseuille's law), with vasodilation the VSM would need to contract 8.8% more in hypercapnia, compared to hypocapnia, to restore flow to its original level, also assuming that the BP change is the same in both cases. When one notes that for the same extremes of mean $PaCO_2$, F_{upLim} is 56% lower in hypercapnia, compared to hypocapnia (Table 2), then it does not look plausible that the VSM shortening hypothesis could provide the complete explanation for the changes in F_{upLim} with $PaCO_2$. Secondly, and much more plausible, are the alterations in pH resulting from changes in $PaCO_2$. VSM studies *in vitro* have shown that changes in extracellular pH affect endothelial function and intracellular nitric oxide (Capellini *et al.*, 2013), as well as calcium influx, but not intracellular calcium release (Nazarov *et al.*, 2000). Of particular relevance, reducing pH also reduced the rate of VSM shortening in the rat portal vein (Peiper *et al.*, 1976) which would have a direct link to the reduced F_{upLim} we found with hypercapnia. Nevertheless, further studies are needed to replicate these results in cerebral VSM preparations, ideally using stimuli that could help to infer the link between extracellular pH and F_{upLim}. BP variability could also be proposed as a determinant of F_{upLim} since it would be expected to increase with hyperventilation, when the highest values of F_{upLim} were observed (Table 2). However, as shown by the PSD in Fig. 5, this is not plausible since hypercapnia led to similar or higher values of PSD compared to normocapnia and hypocapnia, despite showing the lowest values of F_{upLim}.

Methodological aspects

Different methodological approaches have been adopted in experimental work on the frequency domain properties of dynamic CA. In rats, Kolb and colleagues (Kolb *et al.*, 2007) performed a very elegant study using periodic occlusion of the aorta at eight different frequencies to induce changes in BP. By comparing the response of gain with and without nifedipine, they concluded that dynamic CA was limited to a maximum frequency of 0.1 Hz. Unfortunately, this conclusion failed to consider the essential role of phase. In their communication, it is possible to observe that the differences between control conditions, and inhibition of the myogenic response with nifedipine, ceased around 0.1 Hz for normalised gain, but for phase significant differences extended to approximately 0.25 Hz, which would be closer to our findings. In anaesthetised and intubated neonatal swine, Fraser and colleagues (Fraser III *et al.*, 2013) induced periodic changes in BP by modulation of the positive end-expiratory pressure. Instead of the phase between BP and CBF, they analysed the phase between BP and intracranial pressure, assuming that dynamic CA was exhausted

when the phase difference approached zero. Although these investigators did not make direct reference to an upper frequency limit, their results show that phase reaches a minimum at frequencies somewhere in between 0.1 and 0.25 Hz. In the intact human, phase frequency response estimates have been reported from a multitude of studies. Without exception, whilst the amplitude ('gain') frequency response tends to increase with frequency, the phase drops to near zero or shows small negative values in the range 0.1-0.3 Hz. In population averaged curves, the reduction of phase with frequency is more gradual, but in individual estimates, as represented in Fig. 1, it is difficult to detect the exact frequency where phase should be considered for detection of F_{upLim}. As an alternative, the method we adopted, of gradually zeroing the phase from 0.5 Hz, down to 0.01 Hz presents a much more robust approach that allowed identification from the *ARI(f)* curve, by means of segmental bi-linear regression. To destroy the frequency pattern of gain though, the exact similar approach cannot be adopted as it leads to instability in the inverse fast Fourier transform needed to obtain the CBFV step response (Fig. 2). Nevertheless, the gain pattern is equally destroyed by gradual replacement with a constant value, as long as this is greater than zero. As demonstrated, this did not have an effect on the CBFV step response temporal pattern or ARI values (Fig. 2).

The finding that F_{upLim} has considerable inter-subject variability and is highly dependent on $PaCO_2$, has considerable methodological implications for the assessment of dynamic CA. First of all, further studies are needed to investigate the diagnostic and prognostic potential of the entire *ARI(f)* curve (Figs. 2 & 3) as a new paradigm for quantification of CA effectiveness in humans. In particular, testing the hypothesis that F_{upLim}, and its dependence on $PaCO_2$, might be altered in disease states would be of considerable interest. Secondly, our findings question the physiological basis for compartmentalising the frequency response of dynamic CA into different frequency bands, such as the VLF, LF and HF bands that have been used extensively in physiological and clinical studies (Zhang *et al.*, 1998; Claassen *et al.*, 2016). The range of F_{upLim} values that we estimated (Table 2) suggest that averaging values of phase and gain in the LF interval (0.07-0.20 Hz) can lead to severe distortions, by including 'rogue' values outside the limits of dynamic CA. Similar conclusions were reached by a different study based on the properties of the coherence function, also showing that the 0.07 Hz break point was not justified as a meaningful separation of two distinct frequency bands (Panerai *et al.*, 2018). Above all, the demonstration that F_{upLim} is closely associated with $EtCO_2$ (Fig. 4) adds to our understanding of the physiology of dynamic CA in humans, providing a more

sound explanation to previous empirical observations of the effects of $PaCO_2$ on the CBFV speed of response to sudden changes in BP (Aaslid *et al.*, 1989; Panerai *et al.*, 1999; Minhas *et al.*, 2018). For this reason, and the potential associations to phenotype, as shown by the high inter-subject variability of F_{upLim}, we would argue that further progress on physiological and clinical studies of CBF regulation in humans would benefit from abandoning the use of parameters averaged over the VLF, LF and HF frequency bands, that lack specific physiological interpretation and can hide more than they reveal about the underlying mechanisms of dynamic CA.

Limitations

CBFV can only reflect changes in CBF if the diameter of the insonated vessel (MCA) remains constant, a condition that is less likely to be met at high levels of hypercapnia (Coverdale *et al.*, 2014; Verbree *et al.*, 2014). In our case, any changes in MCA diameter that might have taken place with the breathing of 8% CO_2 in air would lead to an underestimation of the changes in CBF with hypercapnia (Table 1). However, despite these differences, all other parameters from the study would not be affected, as ARI is independent of amplitude factors.

Of the 41 subjects that were recruited, 17 were rejected due to the estimation process for ARI not meeting the necessary statistical requirements (Panerai *et al.*, 2016). At first glance, this relatively high number of subjects removed from the study might suggest poor quality data, which was not the case. Given that ARI was obtained for both hemispheres, for five different conditions, in total there were 410 estimates. Any subject without the complete set of 10 estimates of ARI was removed, to allow a perfectly balanced comparison of the effects of hemisphere, as well as $PaCO_2$. This rigorous approach is highly recommended in dynamic CA studies, given the large inter-subject variability of parameters like ARI, phase or gain, which could lead to distorted results when comparing repeated measures with unbalanced groups of subjects.

Hypercapnia was induced by subjects breathing 5% or 8% CO_2 in air during two minutes, preceded and followed by 90 s of normal breathing. To obtain the estimates of phase needed to estimate F_{upLim} though, we needed to include the entire 5 min recording, which led to the relatively low values of mean $EtCO_2$ given in Table 1. In fact, considering only the last 30 s of the manoeuvre, the population mean values would be 44.2 ± 5.1 and 48.5 ± 7.0 mmHg, for

the 5 % and 8% CO_2 in air manoeuvres, respectively. Additionally, the potential for an overshoot was higher if $EtCO_2$ at -10mmHg was targeted first by randomized order. This was attributed to vasoconstrictive stimuli leading to a delay before baseline CBFV could be established and therefore further stimuli assessed, despite the set washout period of a minimum of 2 minutes being applied. However, it should also be stated that the magnitude of the change in end-tidal PCO_2 during a fixed fractional inspired CO_2 ($FICO_2$) stimulus is very dependent on the ventilatory drive. In other words, those who ventilate much more for a given $FICO_2$ stimulus will typically have less of an increase in $EtCO_2$ than those who have a blunted ventilatory drive. As such, normal variability in $EtCO_2$ values (which can be quite large) are normally experienced during $FICO_2$ steps. This study did not assess ventilatory drive and hence the influence of such variability.

Although our study did not show significant differences between males and females, for the dependency of F_{upLim} on $EtCO_2$ (Fig. 4), the trend in the absolute value of the slope of females, compared to males ($p=0.108$), might reflect limitations in statistical power that would warrant further studies with larger sample sizes.

Finally, it is important to emphasize that our findings are limited to resting baseline conditions, where the *ARI(f)* was estimated from spontaneous fluctuations in BP and CBFV. During exercise or different protocols for assessment of dynamic CA, such as repeated squat-standing (Claassen *et al.*, 2009; Smirl *et al.*, 2015), it is likely that different values of F_{upLim} could be found. For this reason, further studies of the F_{upLim} parameter under different physiological conditions would be of considerable interest.

CONCLUSIONS

A new paradigm was proposed for characterising the dynamic CA response of healthy human subjects, showing that the pattern of changes of ARI with gradual destruction of the phase frequency response can identify the upper frequency limit (F_{upLim}) at which the CA mechanism can respond to disturbances in mean BP. The strong association of F_{upLim} with $EtCO_2$ changes induced by different breathing manoeuvres suggest that F_{upLim} might reflect alterations in the dynamics of VSM resulting from changes in extracellular pH. Further experimental work is needed to identify the determinants of F_{upLim} and to investigate its potential as a marker of cerebrovascular disease.

Table 1. Physiological characteristics of the population studied for five distinct breathing conditions (n=24). Values are mean ± SD.

	Hypocapnia -10mmHg	Hypocapnia -5mmHg	Baseline (normocapnia)	Hypercapnia 5%	Hypercapnia 8%	p-value*
CBFV R ($cm.s^{-1}$)	47.0 ± 3.7	47.2 ± 4.0	61.1 ± 3.9	64.9 ±9.4	66.4 ± 11.8	<0.0001
CBFV L ($cm.s^{-1}$)	45.1 ± 3.5	45.9 ± 3.8	56.9 ± 3.7	59.9 ± 8.3	62.6 ± 10.7	<0.0001
Mean BP (mmHg)	86.2 ±6.3	85.6 ± 3.7	88.6 ± 3.2	88.5 ± 4.2	91.1 ± 4.8	0.234
HR (bpm)	65.5 ± 3.6	65.4 ± 3.4	67.2 ± 3.5	67.5 ± 4.1	68.9 ± 4.8	0.020
$EtCO_2$ (mmHg)	28.1 ± 1.9	29.8 ± 1.7	37.9 ± 0.8	40.2 ± 3.4	41.7 ± 5.4	<0.0001
Systolic BP (mmHg)	122.5 ± 9.7	117.5 ± 6.0	121.2 ± 4.9	121.6 ± 6.2	127.2 ± 7.4	0.059
Diastolic BP (mmHg)	69.4 ± 5.1	71.3 ± 3.1	73.5 ± 2.9	73.6 ± 3.5	74.6 ± 3.9	0.293

*one-way repeated measures ANOVA for differences between five conditions. CBFV R: cerebral blood flow velocity right middle cerebral artery, CBFV L: cerebral blood flow velocity left middle cerebral artery, BP: blood pressure, HR: heart rate, $EtCO_2$: end-tidal carbon dioxide.

Table 2. Autoregulation Index (ARI) and upper frequency limit (F_{upLim}) of dynamic CA for five distinct levels of $PaCO_2$ (n=24). Values are mean ± SD for averaged estimates from the right and left MCAs.

	Hypocapnia -10 mmHg	Hypocapnia -5 mmHg	Normocapnia (baseline)	Hypercapnia 5 % CO_2	Hypercapnia 8 % CO_2	p-value*
ARI	5.68 ± 2.03	5.66 ± 1.71	5.02 ± 1.27	3.19 ± 1.85	2.73 ± 2.29	<0.0001
F_{upLim} (Hz)	0.167 ± 0.036	0.158 ± 0.039	0.122 ± 0.034	0.103 ± 0.036	0.094 ± 0.040	<0.0001

*p-values for the effect of breathing condition (5 levels) from 2-way repeated measures ANOVA. Corresponding p-values for the effects of hemisphere and interaction were non-significant for both parameters. ARI: autoregulation index, F_{upLim}: upper frequency limit, CO_2: carbon dioxide.

Figure legends

Figure 1 – Representative transfer function parameters from a 29 year-old male subject. A. Phase frequency response; B. Amplitude ('gain') frequency response; C. Coherence function. Normocapnia (continuous line) and hypercapnia (8% CO_2 in air, dashed line).

Figure 2 – CBFV step responses and *ARI(f)* from the same subject as in Fig. 1 for gradual destruction of the phase (A & C) and gain (B & D) spectral patterns from the high to the lower frequencies. A. CBFV step responses for the intact phase spectrum (solid line) and to gradual zeroing to 0.20 Hz (dashed line), 0.15 Hz (dotted line), 0.10 Hz (long dashed line) and 0.05 Hz (dash-dotted line). B. CBFV step responses using similar cutoff frequencies for gradual destruction of the gain spectra. C. *ARI(f)* resulting from gradual zeroing of the phase spectra for normocapnia (closed triangles) and hypercapnia (8% CO_2 in air, open circles). Vertical arrows marks the position of F_{upLim} identified using segmental bi-linear regression (dashed lines). D. Corresponding curves of *ARI(f)* for gradual destruction of the gain spectra where it is not possible to identify an upper frequency limit.

Figure 3 – Population mean (continuous line) and ± SE (dashed line) curves for *ARI(f)* for the left (A,C,E,G,I) and right (B,D,F,H,J) MCA. (A,B) Hypocapnia targeted at -10 mmHg from baseline; (C,D) hypocapnia targeted at -5 mmHg from baseline; (E,F) Normocapnia (baseline); (G,H) hypercapnia (5% CO_2 in air); and (I,J) hypercapnia (8% CO_2 in air). Vertical arrows indicate the population mean value of F_{upLim} with the horizontal error bars showing the ± SE values.

Figure 4 – Correlation between F_{upLim} and $EtCO_2$ for all five conditions studied (see Methods), showing the linear regression line for females (open circles, continuous line) and males (filled squares, dashed line).

Figure 5 – Power density spectra of CBFV (solid line) and BP (dashed line) in logarithmic scale for five levels of $PaCO_2$. A. Hypocapnia (-10 mmHg target); B. Hypocapnia (-5 mmHg target); C. Normocapnia (baseline); D. Hypercapnia (5 mmHg); E. Hypercapnia (8 mmHg). Note different amplitude scale in A. The error bars correspond to the largest + 1 SE at the frequency of occurrency. The vertical arrows mark the position of the mean F_{upLim}, translated from Table 2.

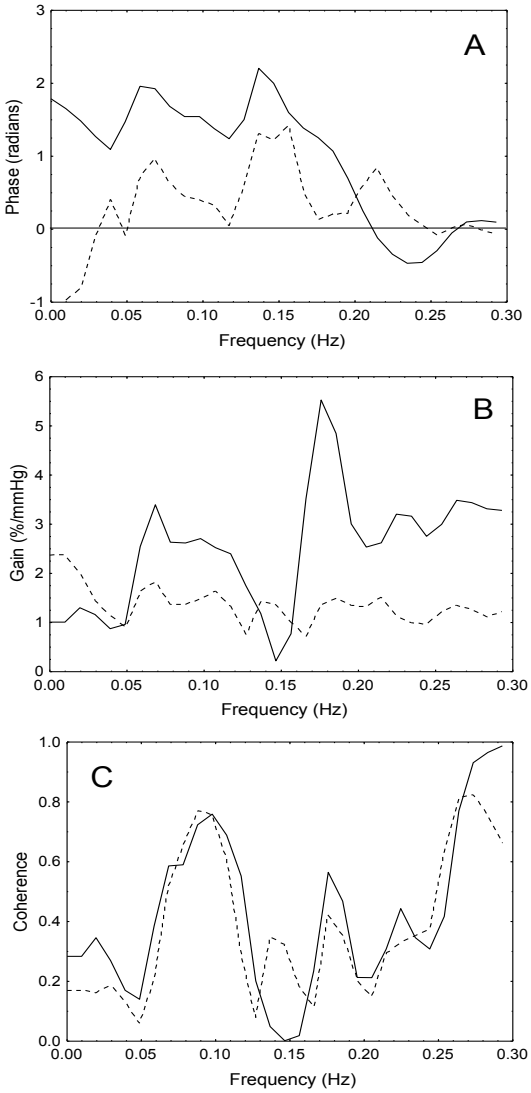

Figure 1 – Representative transfer function parameters from a 29 year-old male subject. A. Phase frequency response; B. Amplitude ('gain') frequency response; C. Coherence function. Normocapnia (continuous line) and hypercapnia (8% CO_2 in air, dashed line).

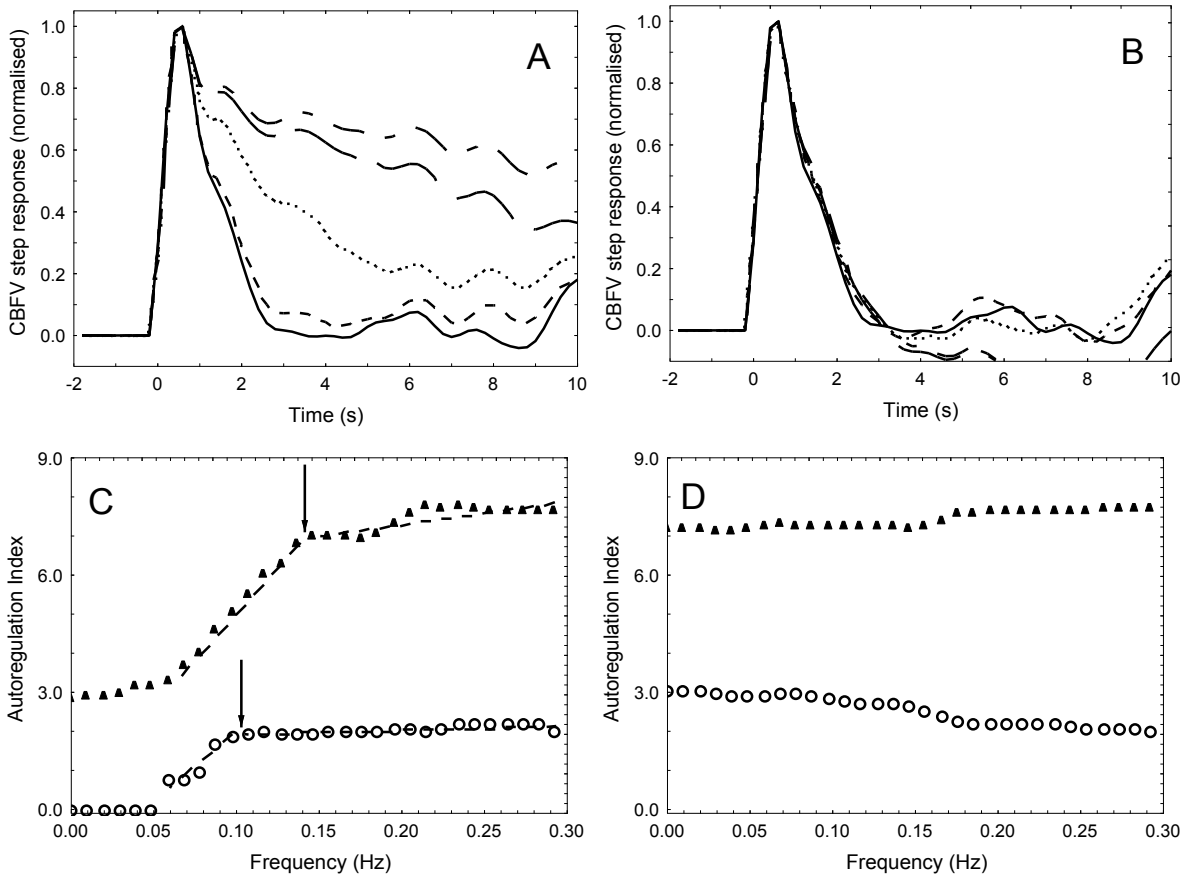

Figure 2 – CBFV step responses and *ARI(f)* from the same subject as in Fig. 1 for gradual destruction of the phase (A & C) and gain (B & D) spectral patterns from the high to the lower frequencies. A. CBFV step responses for the intact phase spectrum (solid line) and to gradual zeroing to 0.20 Hz (dashed line), 0.15 Hz (dotted line), 0.10 Hz (long dashed line) and 0.05 Hz (dash-dotted line). B. CBFV step responses using similar cutoff frequencies for gradual destruction of the gain spectra. C. *ARI(f)* resulting from gradual zeroing of the phase spectra for normocapnia (closed triangles) and hypercapnia (8% CO_2 in air, open circles). Vertical arrows marks the position of F_{upLim} identified using segmental bi-linear regression (dashed lines). D. Corresponding curves of *ARI(f)* for gradual destruction of the gain spectra where it is not possible to identify an upper frequency limit.

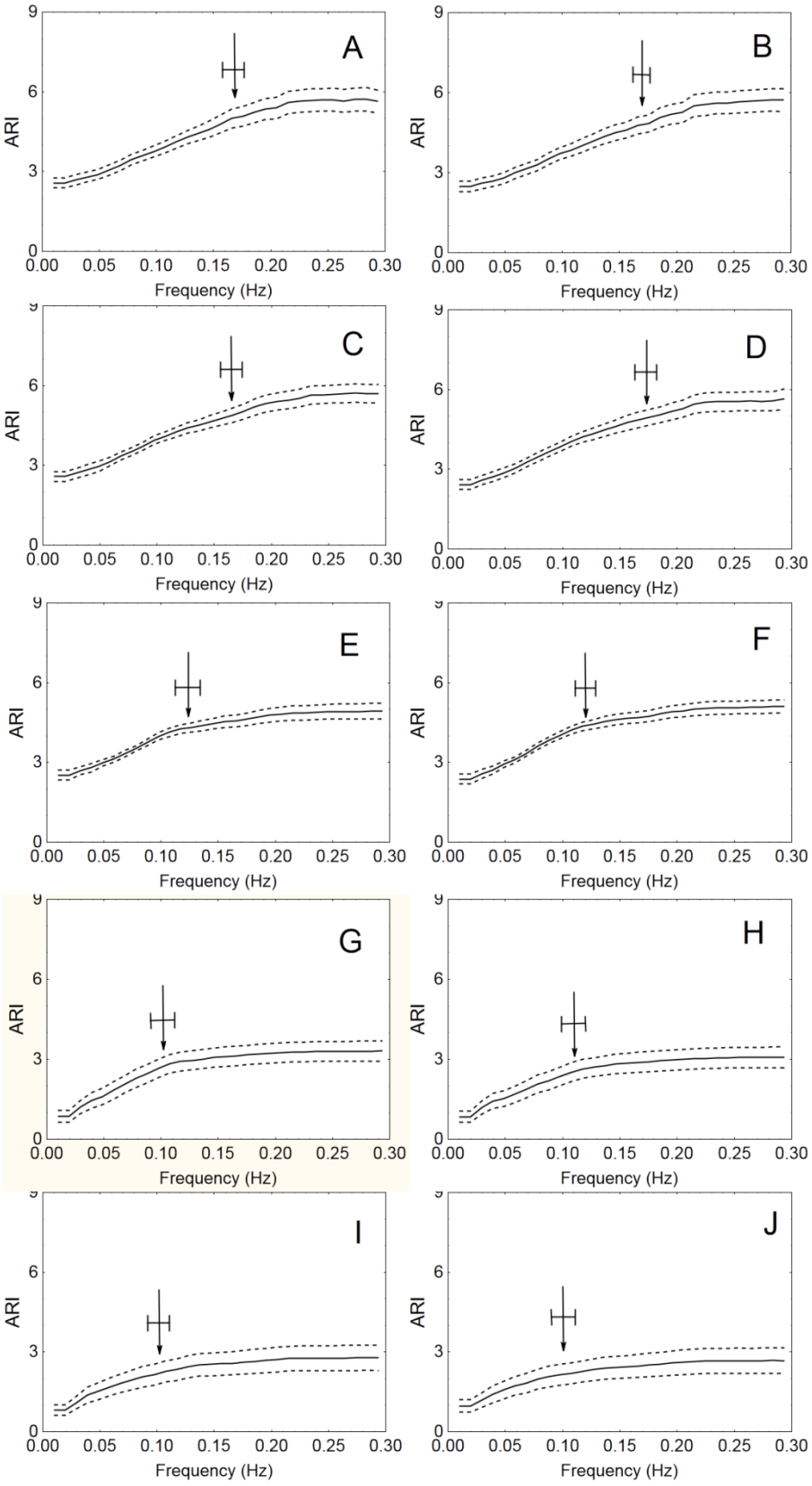

Figure 3 – Population mean (continuous line) and ± SE (dashed line) curves for *ARI(f)* for the left (A,C,E,G,I) and right (B,D,F,H,J) MCA. (A,B) Hypocapnia targeted at -10 mmHg from baseline;

(C,D) hypocapnia targeted at -5 mmHg from baseline; (E,F) Normocapnia (baseline); (G,H) hypercapnia (5% CO_2 in air); and (I,J) hypercapnia (8% CO_2 in air). Vertical arrows indicate the population mean value of F_{upLim} with the horizontal error bars showing the ± SE values.

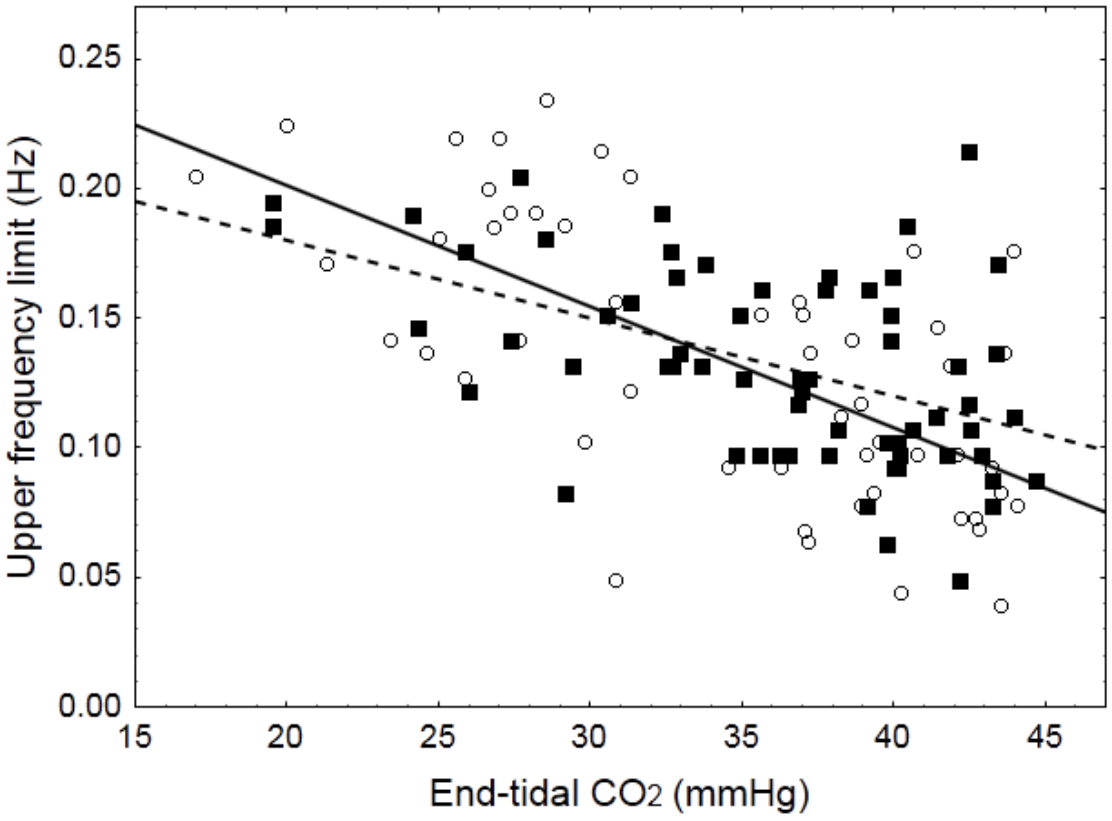

Figure 4 – Correlation between F_{upLim} and $EtCO_2$ for all five conditions studied (see Methods), showing the linear regression line for females (open circles, continuous line) and males (filled squares, dashed line).

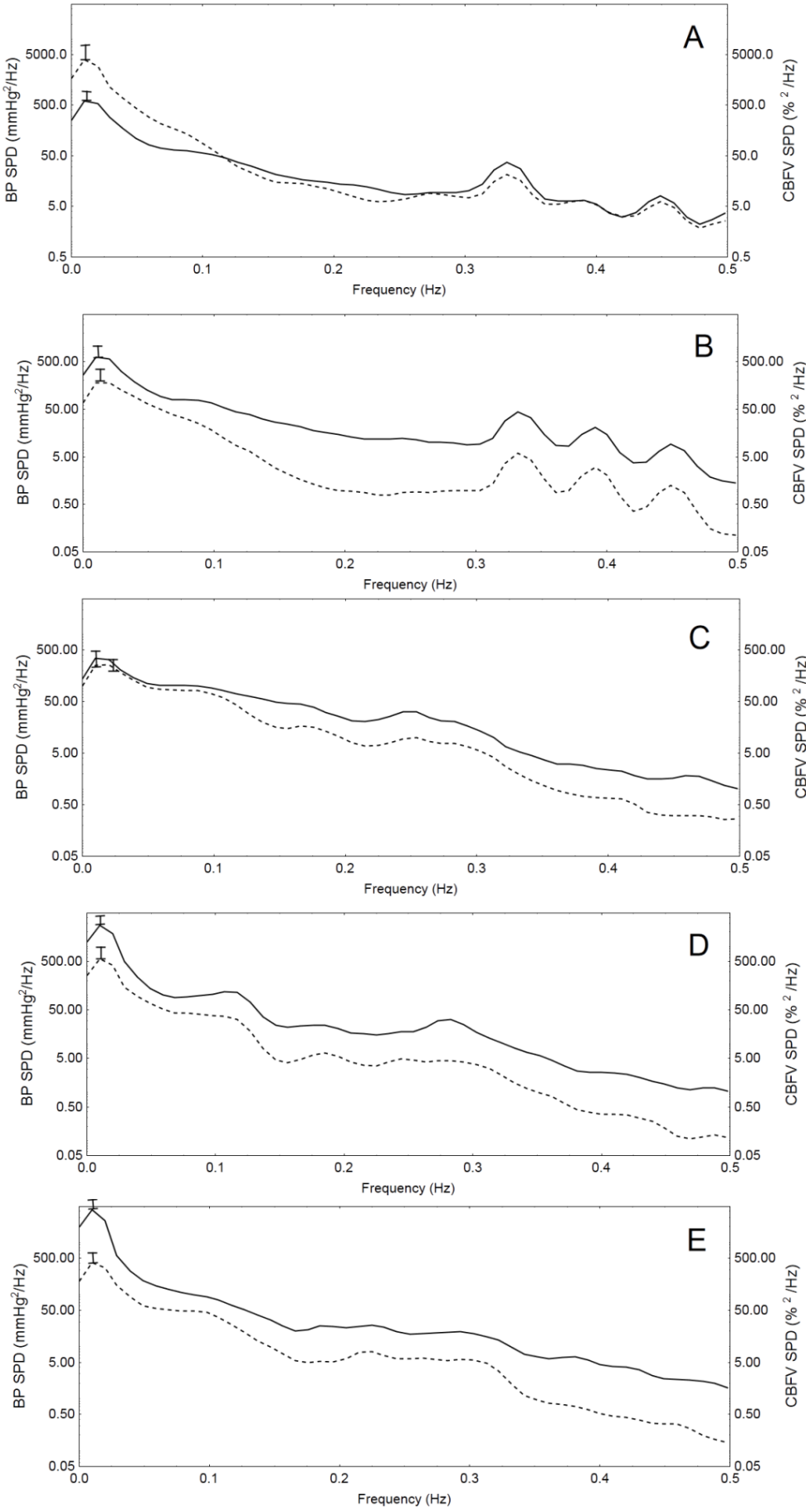

Figure 5 – Power density spectra of CBFV (solid line) and BP (dashed line) in logarithmic scale for five levels of $PaCO_2$. A. Hypocapnia (-10 mmHg target); B. Hypocapnia (-5 mmHg target); C. Normocapnia (baseline); D. Hypercapnia (5 mmHg); E. Hypercapnia (8 mmHg). Note different amplitude scale in A. The error bars correspond to the largest + 1 SE at the frequency of occurrency. The vertical arrows mark the position of the mean F_{upLim}, translated from Table 2.

REFERENCES

Aaslid R, Lindegaard KF, Sorteberg W & Nornes H. (1989). Cerebral autoregulation dynamics in humans. *Stroke* **20,** 45-52.

Aaslid R, Markwalder TM & Nornes H. (1982). Noninvasive transcranial Doppler ultrasound recording of flow velocity in basal cerebral arteries. *Journal of Neurosurgery* **57,** 769-774.

Bendat JS & Piersol AG. (1986). *Random Data Analysis and Measurement Procedures*. John Wiley & Sons, New York.

Capellini VK, Restini CBA, Bendhack LM, Evora PRB & Celotto AC. (2013). The effect of extracelular pH changes on intracellular pH and nitric oxide concentration in endothelial and smooth muscle cells from rat aorta. *PLOS One* **8,** e62887.

Claassen JA, Levine BD & Zhang R. (2009). Dynamic cerebral autoregulation during repeated squat-stand maneuvers. *Journal of Applied Physiology* **106,** 153-160.

Claassen JAHR, Meel-van den Abeelen ASS, Simpson DM & Panerai RB. (2016). Transfer function analysis of dynamic cerebral autoregulation: a white paper from the International Autoregulation Research Network (CARNet). *Journal of Cerebral Blood Flow and Metabolism* **36,** 665-680.

Cooke WH, Hoag JB, Crossman AA, Kuusela TA, Tahvanainen KUO & Eckberg DL. (1999). Human responses to uptright tilt: a window on central autonomic integration. *Journal of Physiology* **517.2,** 617-628.

Coverdale NS, Gati JS, Opalevych O, Perrotta A & Shoemaker JK. (2014). Cerebral blood flow velocity underestimates cerebral blood flow during models hypercapnia and hypocapnia. *Journal of Applied Physiology* **117,** 1090-1096.

Drummond JC. (2019). Blood Pressure and the Brain: How Low Can You Go? *Anesthesia & Analgesia* **128,** 759-771.

Fraser III CD, Brady KM, Rhee CJ, Easley RB, Kibler KK, Smieleswski P, Cznosnyka M, Kaczka DW, Andropoulos DB & Rusin C. (2013). The frequency response of cerebral autoregulation. *Journal of Applied Physiology* **115,** 52-56.

Giller CA. (1990). The frequency-dependent behavior of cerebral autoregulation. *Neurosurgery* **27,** 362-368.

Heistad DD & Kontos HA. (1983). Cerebral Circulation, in Handbook of Physiology section 2 *The Cardiovascular System* vol. III, *Peripheral Circulation and Organ Blood Flow* part 1 . *American Physiological Society, Washington DC*.

Hoiland RL, Fisher JA & Ainslie PN. (2019). Regulation of the Cerebral Circulation by Arterial Carbon Dioxide. *Comprehensive Physiology* **9,** 1101-1154.

Hughson RL, Edwards MR, O'Leary DD & Shoemaker JK. (2001). Critical analysis of cerebrovascular autoregulation during repeated head- up tilt. *Stroke* **32,** 2403-2408.

Karemaker JM. (1999). Autonomic integration: the physiological basis of cardiovascular variability. *Journal of Physiology* **517.2,** 316.

Kolb B, Rotella DL & Stauss HM. (2007). Frequency response characteristics of cerebral blood flow autoregulation in rats. *American Journal of Physiology* **292,** 432-438.

Lassen NA. (1959). Cerebral blood flow and oxygen consumption in man. *Physiological Reviews* **39,** 183-238.

Minhas JS, Panerai RB & Robinson TG. (2018). Modelling the cerebral haemodynamic response in the physiological range of $PaCO_2$. *Physiological Measurement* **39,** 1-11.

Minhas JS, Kennedy C, Robinson TG & Panerai RB. (2019). Different strategies to initiate and maintain hyperventilation: their effect on continuous estimates of dynamic cerebral autoregulation. *Physiological Measurement* **40**:015003.

Nazarov V, Aquino-DeJesus A & Apkon M. (2000). Extracellular pH, Ca2+ influx and response of vascular smooth muscle cells to 5-hydroxytryptamine. *Stroke* **31,** 2500-2507.

Panerai RB. (2004). System identification of human cerebral blood flow regulatory mechanisms. *Cardiovascular Engineering* **1,** 59-71.

Panerai RB. (2008). Cerebral autoregulation: From models to clinical applications. *Cardiovascular Engineering* **8,** 42-59.

Panerai RB, Deverson ST, Mahony P, Hayes P & Evans DH. (1999). Effect of CO_2 on dynamic cerebral autoregulation measurement. *Physiological Measurement* **20,** 265-275.

Panerai RB, Haunton VJ, Minhas JS & Robinson TG. (2018). Inter-subject analysis of transfer function coherence in studies of dynamic cerebral autoregulation. *Physiological Measurement* **39,** 125006.

Panerai RB, Haunton VJ, Salinet ASM & Robinson TG. (2016). Statistical criteria for estimation of the cerebral autoregulation index (ARI) at rest. *Physiological Measurement* **37,** 661-680.

Panerai RB, Hudson V, Fan L, Mahony P, Yeoman PM, Hope T & Evans DH. (2002). Assessment of dynamic cerebral autoregulation based on spontaneous fluctuations in arterial blood pressure and intracranial pressure. *Physiological Measurement* **23,** 59-72.

Panerai RB, Kelsall AWR, Rennie JM & Evans DH. (1996a). Analysis of cerebral blood flow autoregulation in neonates. *IEEE Transactions on Biomedical Engineering* **43,** 779-788.

Panerai RB, Kelsall AWR, Rennie JM & Evans DH. (1996b). Mechanism of cerebral autoregulation in neonates. *Early Human Development* **47,** 206-207.

Paulson OB, Strandgaard S & Edvinson L. (1990). Cerebral autoregulation. *Cerebrovascular and Brain Metabolism Reviews* **2,** 161-192.

Peiper U, Ehl M, Johnson U & Laven R. (1976). Force-velocity relations in vascular smooth muscle: The influence of pH, pCA and noradrenaline. *Pflugers Arch* **364,** 135-141.

Sammons EL, Samani NJ, Smith SM, Rathbone WE, Bentley S, Potter J & Panerai RB. (2007). Influences of noninvasive peripheral arterial blood pressure measurements on assessment of dynamic cerebral autoregulation. *Journal of Applied Physiology* **103,** 369-375.

Simpson D & Claassen J. (2018). CrossTalk opposing view: dynamic cerebral autoregulation should be quantified using induced (rather than spontaneous) blood pressure fluctuations. *Journal of Physiology* **596,** 7-9.

Smirl JD, Hoffman K, Tzeng YC, Hansen A & Ainslie PN. (2015). Methodological comparison of active- and passive-driven oscillations in blood pressure; implications for the assessment of cerebral pressure-flow relationships. *Journal of Applied Physiology* **120,** 552-563.

Tiecks FP, Lam AM, Aaslid R & Newell DW. (1995). Comparison of static and dynamic cerebral autoregulation measurements. *Stroke* **26,** 1014-1019.

Tzeng YC & Panerai RB. (2018). CrossTalk proposal: dynamic cerebral autoregulation should be quantified using spontaneous blood pressure fluctuations. *Journal of Physiology* **596,** 3-5.

Verbree J, Bronzwaer ASGT, Ghariq E, Versluis MJ, Daemen MJAP, van Buchem MA, Dahan A, van Lieshout JJ & van Osch MJP. (2014). Assessment of middle cerebral artery diameter during hypocapnia and hypercapnia in humans using ultra-high-field MRI. *Journal of Applied Physiology* **117,** 1084-1089.

Willie CK, Tzeng YC, Fisher JA & Ainslie PN. (2014) Integrative regulation of human brain blood flow. *Journal of Physiology* **592**, 841-859.

Zhang R, Behbehani K, Crandall CG, Zuckerman JH & Levine BD. (2001). Dynamic regulation of heart rate during acute hypotension: new insight into baroreflex function. *American Journal of Physiology* **280,** H407-H419.

Zhang R, Zuckerman JH, Giller CA & Levine BD. (1998). Transfer function analysis of dynamic cerebral autoregulation in humans. *American Journal of Physiology* **274,** H233-H241.

Additional information

Competing interests

The authors declared no potential conflicts of interest with respect to the research, authorship, and/or publication of this article.

Author Contributions

RBP, TGR and JSM conceived and designed the study. JSM performed the experiments. JSM and RBP performed data analysis. JSM, RBP wrote the manuscript. RBP, TGR and JSM revised and approved the final version of the manuscript. The data that support the findings of this study are available from the corresponding author (jm591@le.ac.uk) upon reasonable request.

Funding

JSM was funded by a Dunhill Medical Trust Research Training Fellowship (RTF97/0117) and is currently an NIHR Clinical Lecturer in Older People and Complex Health Needs. TGR is an NIHR Senior Investigator.

Acknowledgements

We thank the subjects and their families for their willingness to participate. This work falls under the portfolio of research conducted within the NIHR Leicester Biomedical Research Centre.

Ronney B. Panerai is an Emeritus Professor, Department of Cardiovascular Sciences, University of Leicester and Leicester NIHR Biomedical Research Centre in Cardiovascular Disease, Glenfield Hospital, Leicester, UK. His primary research interest is physiological modelling, particularly in the context of cerebral blood flow regulation.